

ON THE EXPERIMENTAL DETERMINATION OF THE MEASUREMENT VOLUME DIAMETER IN THE PDA TECHNIQUE

E. Palacios *, A. Lecuona °, P. A. Rodríguez °

* E.U.I.T.I., Universidad Politécnica de Madrid, Ronda de Valencia, 3. 28012 Madrid. Spain.
e-mail: mepalaci@mi.upm.es

° E.P.S., Universidad Carlos III de Madrid, Avda. de la Universidad, 30. 28911 Leganés. Madrid. Spain.
e-mail: lecuona@ing.uc3m.es

ABSTRACT

Local measurements provided by the phase Doppler anemometry require the accurate determination of the measurement volume size. On this purpose, some strategies are based on the statistical treatment of the particle transit length distributions of the detected particles. However, these distributions can vary significantly depending on the location of the measuring point in the spray, making hard obtaining accurate results. This work aims at studying what causes transit length modifies, such as the measurement environment and the deviation of the particle trajectory from the measurement direction. In this sense, it is presented a systematic study that shows its variation. Experimental results evidence the existence of certain statistical parameters that seem quite insensitive to be modified. As an extension, the possibility to obtain accurate estimations of the measurement volume size in the vicinity of the mixing layer is investigated.

INTRODUCTION

Multiphase flows play an important role in many applications such as mixing in vessels for the chemical industry, transport of airborne particulates and combustion of sprayed liquid fuels, among others. In these processes, governed by heat and mass transport, the interaction of liquid particles with the continuous phase becomes relevant. In the understanding of the involved mechanisms, it is of grant interest valuating local magnitudes, such as the particle number density and the particle size distribution. In this sense, PDA is a measurement technique capable to provide them. In particular, PDA offers the size and the velocity of the single droplets as passing through a small measurement volume. Particle number density and particle size distribution are then presented as derived magnitudes.

Basically, there are two approaches to compute the droplet number density N_D . In the first approach [1], N_D is defined as the ratio of the counted number of droplets to the total volume swept by them during the acquisition time. A second approach for computing the droplet number density lies on the average residence time of the droplets in the measurement volume [2]. Hence, both approaches require a proper estimation of the measurement volume dimension.

The Gaussian illumination in the measurement volume in addition to the particle size dependent scattering properties causes that the particle size participates in the Doppler signal level. As a consequence, the size of the measurement volume increases with the droplet size. Therefore, the large droplets exhibit a higher probability of being detected. Hence, weighting functions are required for obtaining an unbiased particle size distribution [3]. Thus, for later analysis, the collection of detected particles is arranged into particle size classes, each one with equal measurement volume size allocated. Errors are then expected when the particle size is inaccurate determined.

To sum up, the PDA has the ability to make spatially resolved measurements because of the small dimension of the measurement volume. However, the accurate determination of its size is one of the critical issues in calculating local magnitudes.

For conventional off-axis PDA configuration, quantifying the diameter of the measurement volume belonging to a fixed particle size class requires a single parameter to be determined. A number of algorithms providing in-situ accounting of measurement conditions can be found in the literature [1,4,5]. All of them share the same strategy: the size of the measurement volume is estimated by averaging a certain parameter over the collection of measured signals, assuming the amount of signals is statistically enough. In this sense, each algorithm offers a closed form that relates the obtained average value to the diameter of the measurement volume.

The Saffman procedure [1] makes use of the average square of the transit length of the detected droplets, whereas the transit time method [4] allocates the maximum transit length reached by the particle collection. In complex flows, with non one-dimensional particle trajectories, both strategies require to know the deviation angle of the particle trajectory from the measurement direction. Hence, a suitable correction can be applied. Otherwise, the transit length will become underestimated. In fact, the measured particles are arranged into particle velocity class for later processing. On the contrary, Sommerfeld and Qiu [5] rely more on the maximum amplitude of the signal. This latter avoid the effect of the direction of the droplet trajectory by reprocessing the signal amplitude with an additional trigger level. Thus, it is ahead of the previous methods, avoiding the difficulties that a three-dimensional configured PDA would involve.

The effect of the changeable measurement environment from a location to another within the spray could be turned up critical in dense sprays. Dense sprays are characterized by being optically dense (high N_D) and optically thick (low laser light transmittance). Droplets interposed in the optical light path away from the measurement volume cause the signal amplitude to decrease. Moreover, the light scattered by the particle outside the measurement volume contributes to

increase the background level. In fact, for a fixed particle size and a preset particle trajectory, a variety of signal amplitude and signal to noise ratio is expected. For severe measurement environment, the requirements of PDA sensitivity (set by the power illumination and the photomultiplier voltage, among others) can even change.

The present paper is focused at studying the effect of the spray dynamics and of the measurement environment on the estimation of the size of the measurement volume. Since this last is consequent with a statistical process, it is of interest studying how the changes in the original data distribution influence on the resulting statistical parameter. This work is restricted to the information provided by the available Doppler signal processor. Hence, only the particle transit length distributions have been examined. The effect of measurement conditions owing to dense sprays on the particle transit length distributions is carefully examined. Particularly, this work aims at investigate the existence of parameters able to provide a more robust estimation of the size of the measurement volume using a one-dimensional configured PDA.

EXPERIMENTAL SETUP

Figure 1 sketches the experimental setup used in this work. Measurements have been carried out in solid cone water sprays issued from an axis-symmetrical coaxial air-blast injector. The injector assembly was mounted on a two-dimensional traverse mechanism in open quiescent atmosphere. The traverse system, a step motor driven by computer software, allows the complete spatial characterization of the spray on the measuring plane, located 110 mm downstream the injector nozzle. At this distance 1-D spherical droplet motion in the z direction is assured, excepting the external mixing layer. A fan provides air suction to the bottom of the spray to avoid additional spray flow recirculation.

A standard single-component phase Doppler analyzer (Dantec Dynamics) provides the PDA measurements. A multimode argon-ion laser (Coherent Innova 310) supplies the PDA illumination. The transmitting fiber optics is coupled to the laser beam conditioning optics. Two laser beam, 514 nm wavelength light, separated 40 mm at the PDA emitter front lens, meet at the waist of 96.8 μm Gaussian diameter d_g (e^{-2} intensity), where the measurement volume locates. The receiving optics is placed at 73° to the forward scattering direction. The photomultiplier slit, 100 μm wide, defines the PDA measurement volume as a cylinder slide of diameter d_{ge} and 105 μm long (see the detail in Fig.1). The 57N10 phase Doppler signal processor detects, processes and validates the Doppler signals from the photomultiplier tube detectors. Signal detection is based on a signal amplitude method [6]. The detected signals are processed using a covariance method [6]. Detected droplets are divided into size classes 3 μm wide, for subsequent analysis.

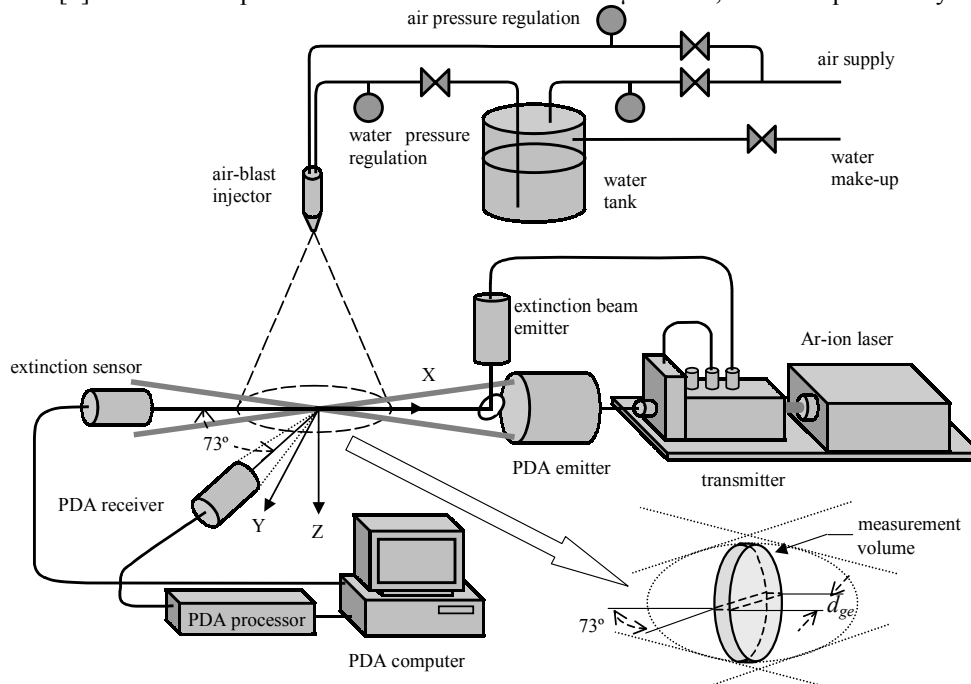


Figure 1: Experimental set-up. The detail shows the PDA measurement volume.

A 488 nm wavelength collimated laser beam, called extinction beam, also supplied by the argon-ion laser, is directed along the x -axis to be coplanar with the PDA illumination beams, overlapping with the PDA measurement volume. A sensor detects the power from the extinction beam after traversing the spray. The collection angle of the sensor is 3.33 mrad, small enough for a range [5, 50 μm] of particle sizes to assure that only the undisturbed beam reaches the sensor. Thus, the extinction sensor provides optical length values that, comparing with the ones calculated from the PDA measurements; lets validate the PDA measurements [7].

EXPERIMENTAL RESULTS AND DISCUSSION

Figure 2 compares the diameters of measurement volume for the 13.5 μm particle size class, resulted of applying the Saffman method and the transit time method in a dilute and a dense spray. For a fixed particle size class, the maximum transit length has been obtained by inspecting the 95% of the detected particles with the smaller transit lengths. The measuring points are located along the $y=0$ line. The peak particle number density, at the central point, reaches $8 \times 10^4 \text{ cm}^{-3}$ in the dilute spray and $2 \times 10^4 \text{ cm}^{-3}$ in the dense spray. At $x = -20 \text{ mm}$, the peak optical length was 0.1 and 0.69 in

the dilute and dense spray, respectively. In both sprays, the particle trajectory does not deviate more than 10° from the measuring direction, excepting the external mixing layer. We note that the estimated diameter changes significantly with the position of the point, whatever the method chosen. Measurement conditions vary considerably along the centerline in the dense spray. The size of the measurement volume decreases with the signal amplitude. Hence, it is expected that the measurement volume diameter reduce as the optical length increases. However, data depicted in Fig. 2 show an ambiguous tendency when comparing data from dilute to dense spray, and when comparing data within the spray. Fixed a particle velocity class, the transit length of the j -th droplet LT_{kj} belonging to the k -th particle size class comes from multiplying its velocity v_{kj} by the time duration of the matching signal TT_{kj} , that is, $LT_{kj} = |v_{kj}| TT_{kj}$. Hence, transit length is sensitive to deviation of the particle trajectory from the measuring direction. However, in both sprays, the deviation that the particles exhibit in the core can be considered negligible. In the following, a close sight to the distributions of the particle transit length is done.

The transit length distribution relating to a preset size class shows the amount of particles in each transit length class. Figure 3 illustrates some statistical parameters that allow describing the spread pattern of the particle transit lengths in the locations showed in the Fig. 2. In the dilute and in the dense spray, we differentiate two regions: one interior characterized by slight changes in median, mode and mean, and another exterior. We note that these statistical show notable differences between favorable and more exigent measurement conditions. In the following, we examine the transit length histograms obtained at the interior and the exterior region from different spray densities

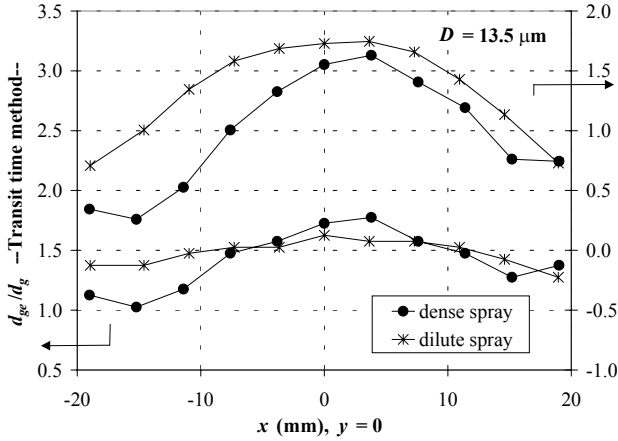


Figure 2: A comparison of the diameter of the measurement volume considering different strategies.

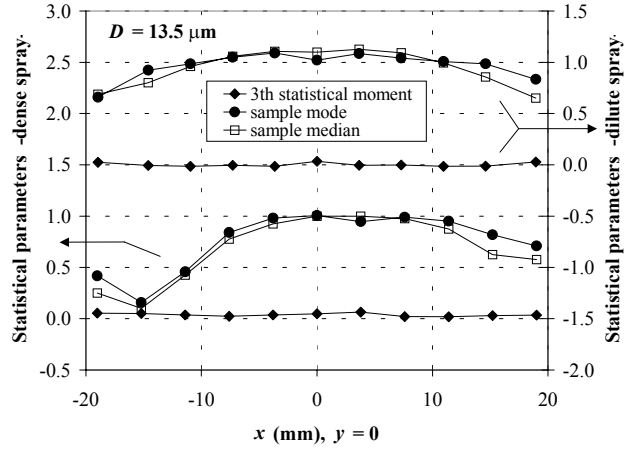


Figure 3: Centerline profiles of several statistical parameters for the particle transit length distribution.

Figure 4 illustrates the histogram obtained from the dilute spray at some interior point, belonging to the $13.5 \mu\text{m}$ particle size class. Assuming that particles have equal probability of crossing any part of the measurement volume, the probability of a certain path length can be predicted [8]. Thus, by inspecting Fig. 4, it is inferred that the enlargement due to background level causes likely that some events exceed the normalized transit length 1.53. As the measuring point moves outside, the histogram appearance changes (Fig. 5). This effect is attributable to the crossing particles. Large scale eddies, typical of the mixing layer, modifies the original trajectory of the particle, which becomes three-dimensional. In fact, we note that the histogram deformation amplify as the particle size decreases. The increase of events matching to the small transit lengths in the external region has been observed in dense spray as well.

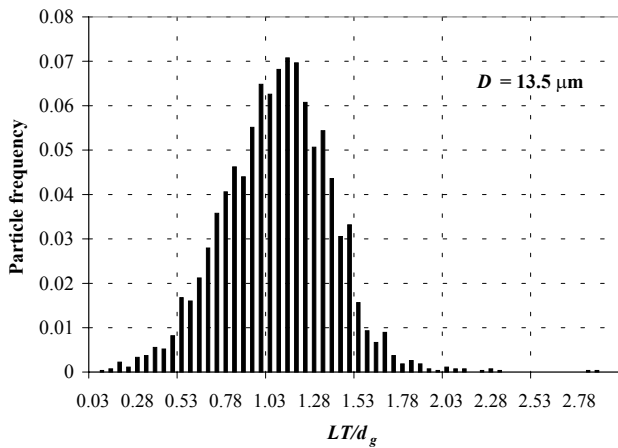


Figure 4: Transit length histogram at some central point of a dilute spray for the $13.5 \mu\text{m}$ particle size class.

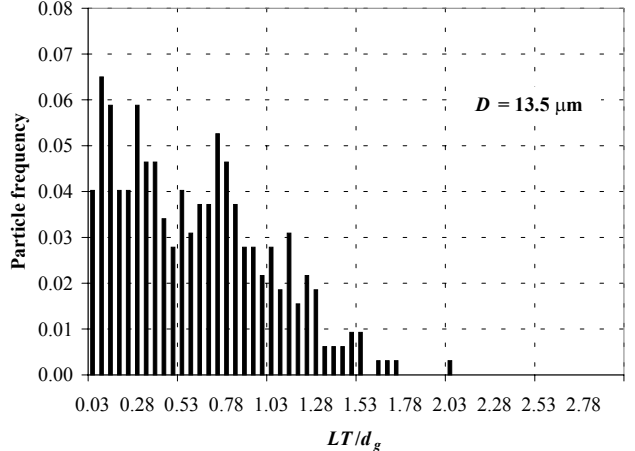


Figure 5: Transit length histogram at some exterior point of a dilute spray for the $13.5 \mu\text{m}$ particle size class.

When spray becomes denser ($\tau = 0.5$, $N_D \sim 6 \times 10^4 \text{ cm}^3$), the frequency of obtaining particles with large transit length increases, as Fig. 6 illustrates. Figure 7 shows the resulting histogram for the central point of the dense spray. The high particle number density and optical length reached ($\tau = 0.65$, $N_D \sim 8 \times 10^4 \text{ cm}^3$) increases noticeably the background

level, as it is inferred from the irregular shape of the histogram. However, note that the sample mode remains unchanged. By comparing the histograms presented in Figs. 4, 6 and 7, it is concluded that the noise affects to a changeable amount of particles, not necessary proportional to the particle number density. Hence, the strategy consisting of fixing the percentage of events not being affected by noise has to solve the handicap of establishing an in-situ cutoff percentage.

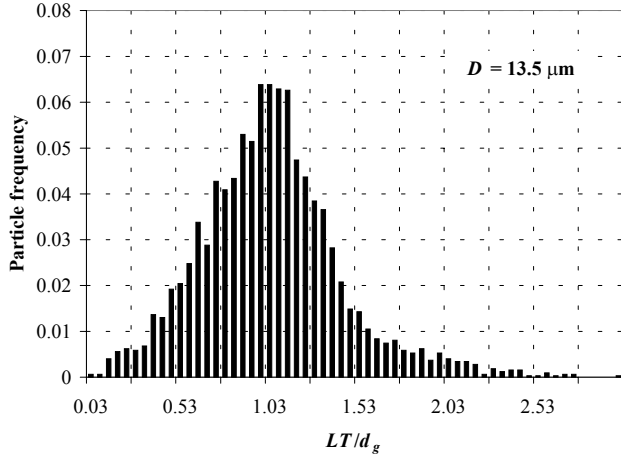


Figure 6: Transit length histogram at an inside point for the 13.5 μm particle size ($\tau = 0.5$, $N_D \sim 6 \times 10^4 \text{ cm}^3$).

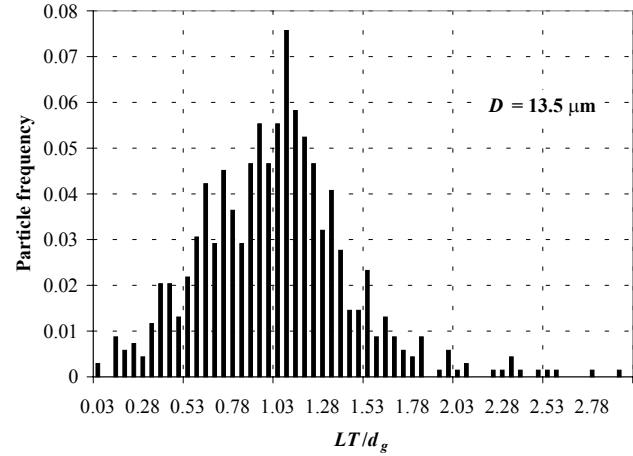


Figure 7: Transit length histogram at an inside point for the 13.5 μm particle size ($\tau = 0.69$, $N_D \sim 8 \times 10^4 \text{ cm}^3$).

Apart from optical noise and the emerging of three-dimensional trajectories that characterizes the mixer layer, there are additional factors capable of modifying the particle transit length histogram. Figure 8 shows the histogram of the point of coordinates $(x, y) = (-15.2, 0)$ mm. This point, placed in the external region, is then subjected to an illuminating path with a high optical length. Note how the smallest transit length is notably more frequent. Such irregularity is attributable to a possible disruption in the illuminating beams caused by the particles located along the illuminating light path. This conjecture explains the returning to normal as the size particle decrease (Fig. 9).

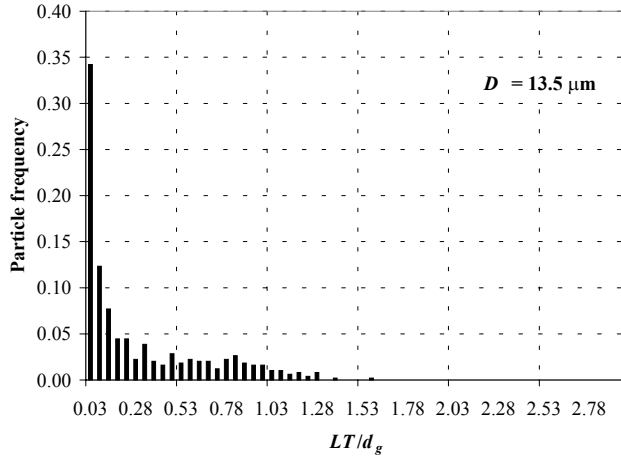


Figure 8: Transit length histogram at the point $(x, y) = (-15.2, 0)$ mm for the 13.5 μm particle size class.

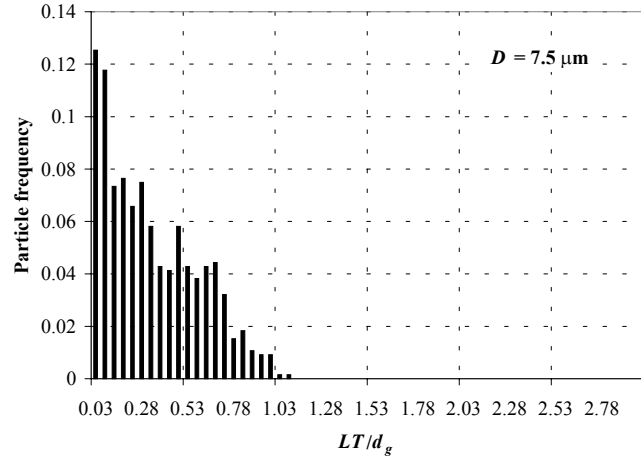


Figure 9: Transit length histogram at the point $(x, y) = (-15.2, 0)$ mm for the 7.5 μm particle size class.

High optical lengths are reached not only in the illuminating path, but also in the receiving path. In fact, the total optical length experienced by any point is obtained adding the illuminating and the receiving optical lengths. Figure 10 depicts the evolution of the optical lengths along an intermediate radius, for a simulated solid cone spray. In the simulation, the spray characteristics were chosen in order to provide τ_{max} close to 0.69. The figure shows a section 165° wide where the total optical length exceeds 0.6. However, the histograms belonging to points located along the receiving light path do not show this effect. Thus, we notice how the points located a few grades far away from the illuminating path recover the normal look as owing to the mixing layer, shown in Fig. 5. Figure 11 lets obtain the piece of the spray that would be affected when only considering the optical length of the illuminating path. This portion reduces when the radius increases, as the experimental data corroborate.

The high optical length in the illuminating path causes the amount of non-validated particles to increase moderately, unless as the spherical deviation it is concerned (Fig. 12). Only when the optical length is high enough, as in $r = 19$ mm, particle rejection involves also particle velocity considerations. It should be noted that, however, the effect on the amount of validated particles in the receiving direction is negligible.

The loss of the coherency of the illuminating beams superimposes to the crossing trajectories effect in the mixing layer, but it can be also noticeable in the internal region of the spray. Figure 13 illustrates the histogram belonging to the 7.5 μm size class. Note that the small particle size alleviates the effect, but it is not removed. In fact, the histogram appears perceptibly distorted; e.g., the normalized sample mode should be equal to 0.82 under favorable measurement

conditions. Therefore, a poor estimation of d_{ge} should be expected at this point.

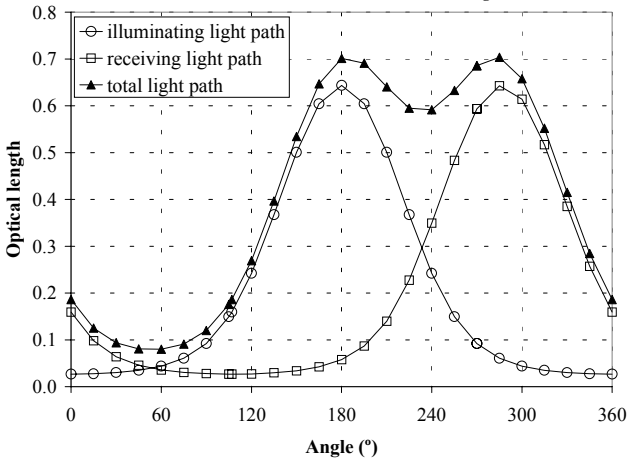


Figure 10: Optical length evolution for a simulated axisymmetric spray ($r = 15.2$ mm; $r_{\max} = 20$ mm).

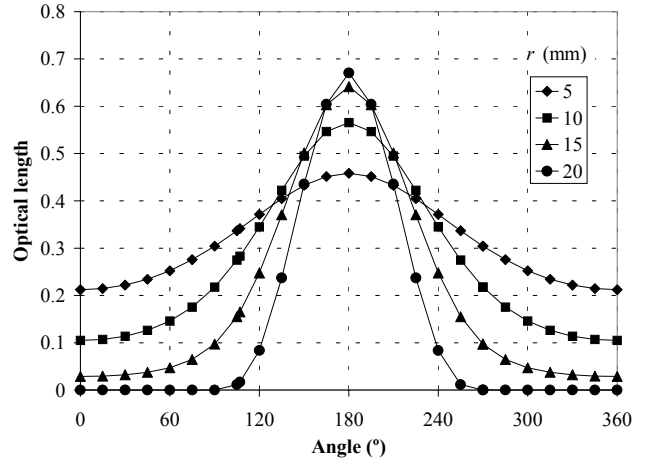


Figure 11: Optical length of the illuminating light path for several radii of a simulated axisymmetric spray

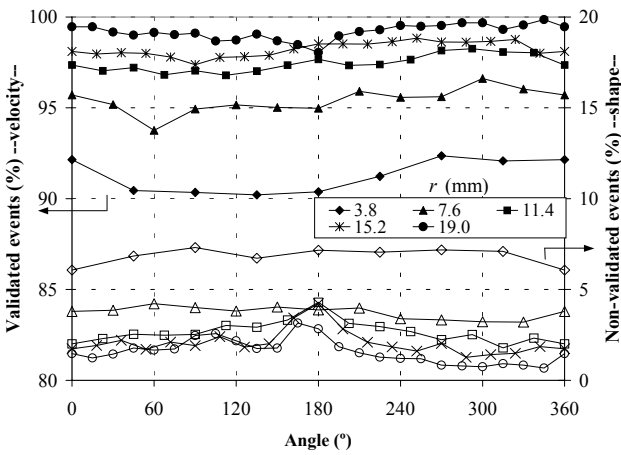


Figure 12: Percentage of validated events according to velocity criterion. From these, percentage of non-validated events according to the spherical deviation.

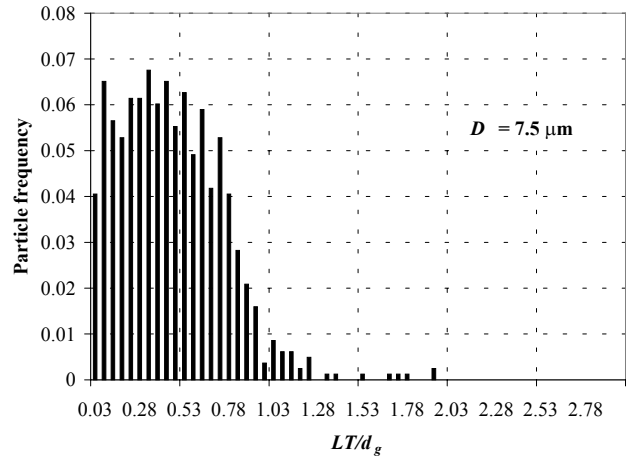


Figure 13: Transit length histogram at the point $(x, y) = (-11.4, 0)$ mm for the $7.5 \mu\text{m}$ particle size.

Let us inspect again the evaluation of the measurement volume diameter that Fig. 2 depicts. In the light of the previous discussion, it may be concluded that the transit time method may provide inaccurate results in noise environments, typical of dense sprays. On the contrary, Saffman procedure seems more affected by the deviation of the particle trajectories from the measurement direction. Therefore, it is worth investigating the existence of some statistical parameter non-being affected by the histogram alteration. Figure 14 compares the distribution of transit lengths measured in the dense spray and in a central point of the dilute spray (Fig. 4), belonging to the $13.5 \mu\text{m}$ particle size class. This figure demonstrates that the account of events remains constant in the central region, excepting the largest transit length classes, enhanced by the optical noise. Figure 15 illustrates similar data, but relating to external points of the dense spray. The different feature is a consequence of the severe change experienced by the histograms.

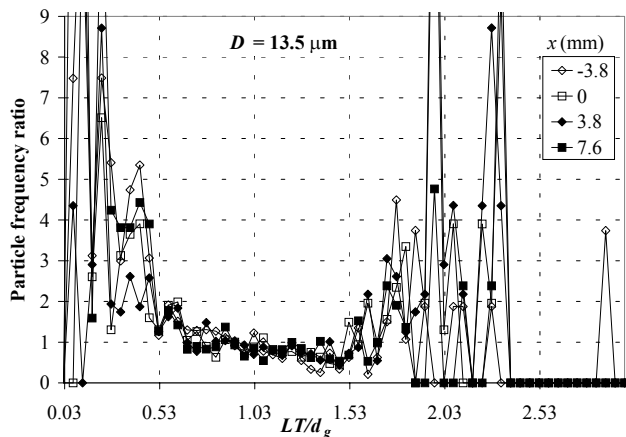


Figure 14: Particle frequency ratio from the dense to the dilute spray at several points in the central region ($y = 0$).

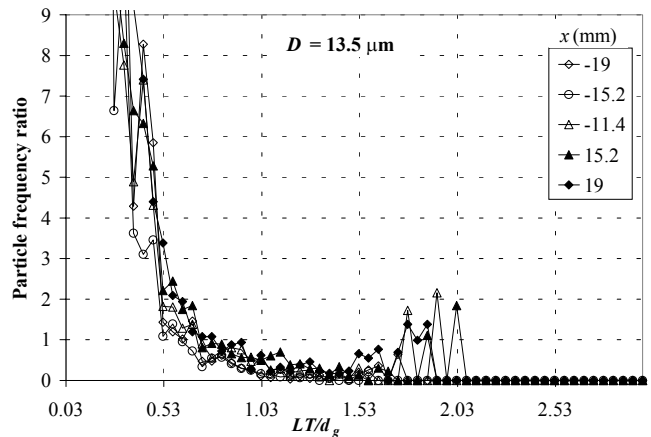


Figure 15: Particle frequency ratio from the dense to the dilute spray at several points in the external region ($y = 0$).

Note that the dimensionless transit length value equal to 0.7 remains unchanged along the whole centerline. This fact can be interpreted as a progressive migration of the particles from the larger to the smaller transit length, as entering the mixing layer.

Figure 16 presents the mode of the transit length distribution along the $y = 0$ line, for the $13.5 \mu\text{m}$ particle size class. By inspecting Fig. 16a, in the light of the previous discussion, two regions are clearly differentiated: in the range $[-15, -15]$ mm of x , the interior region; and up to $x = 15$ mm and down to $x = -15$ mm, the mixing layer. Figure 16b shows how the interior and the external regions are both affected by the illuminating beams disruption (beyond $x = -7.6$ mm). This effect, described by a sharp mode decline, decreases as τ increases. Note that in the interior region, mode seems only affected by the amplitude signal decrease, as a consequence of the increase of the optical length of the measurement environment (Fig. 16a). By comparing the mode value to the accumulated frequency up to the mode, it is inferred from Fig. 16 that the mode is not influenced by possible deviation of the particle trajectories as long as the accumulated frequency does not exceed 10% of that one measured in a one-dimensional dilute spray.

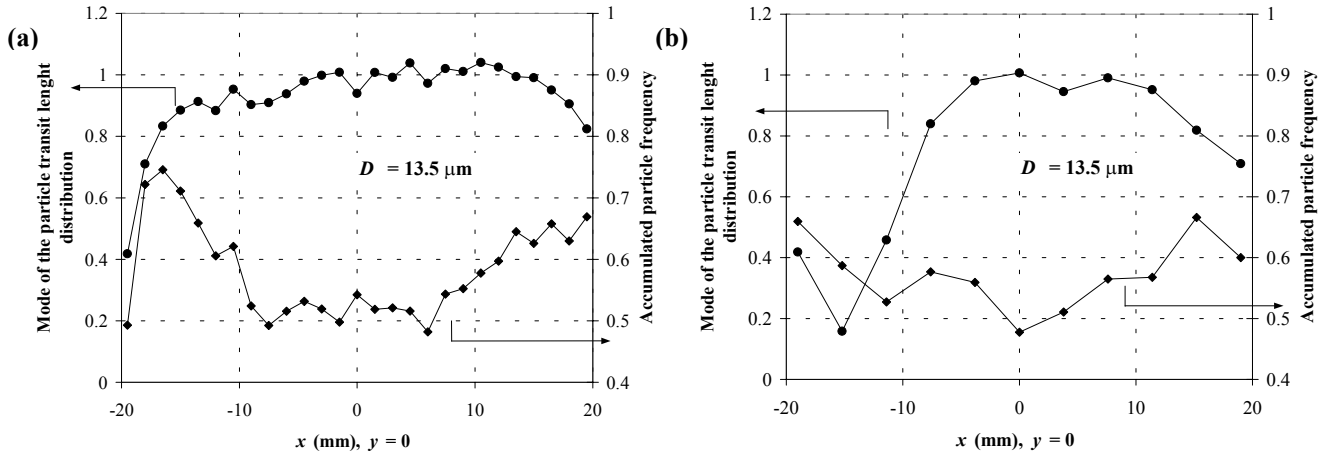


Figure 16: Particle transit length mode and the accumulated particle frequency up to the mode, for the $13.5 \mu\text{m}$ particle size class: (a) $\tau_{\max} = 0.5$, $N_D \sim 6 \times 10^4 \text{ cm}^{-3}$, (b) $\tau_{\max} = 0.69$, $N_D \sim 8 \times 10^4 \text{ cm}^{-3}$.

CONCLUDING REMARKS

The evolution of the transit length distribution in dilute and dense sprays was studied. They have been identified several factors of transit length distribution distortion: the beam disruption caused by the high optical lengths in the illuminating path; the particle trajectory deviation from the measurement direction, characteristic of the mixing layer; and the background level, typical of the high local particle number densities. However, mode is not affected by the high background level. In addition, mode seems not very sensitive to the particle trajectory changes. Moreover, this one lets identify the beam disruption effect. It is concluded that the mode is a suitable parameter for evaluating d_{ge} .

REFERENCES

1. M. Saffman, Automatic calibration of LDA measurement volume size. *Applied Optics*, vol 13, pp 2592-2597, 1987.
2. Y. Hardalupas and A.M.K.P. Taylor, On the measurement of particle concentration near a stagnation point. *Experiments in Fluids*, vol. 8, pp. 113-118, 1989.
3. O. Simonin, A. Deucht, M. Boivin, Large eddy simulation and second moment closure model of particle fluctuating motion in two-phase turbulent shear flows, in Durst F (eds), Selected papers from the 9th Int. Symp. on Turbulent shear flows. Springer, 1995.
4. J.Y. Zhu, R.C. Rudoff, E.J. Bachalo, W.D. Bachalo, Number density and mass flux measurement using the phase Doppler particle analyzer in reacting and non-reacting swirling flows. 31st Aerospace Sciences Meeting & Exhibit. Reno, 1993.
5. M. Sommerfeld and H.-H. Qiu, Particle concentration measurements by phase-Doppler anemometry in complex dispersed two-phase flows. *Experiments in Fluids*, vol. 18, pp. 197-198, 1995.
6. K. Andersen and L. Lading, Burst detection in a phase/frequency processor. 4th Int. Conf. on Laser Anemometry Ohio, 1991.
7. E. Palacios, A. Lecuona, M. de Vega and P.A. Rodriguez, Sensitivity to optical noise of the measurements of particle concentration and volume flux with a phase Doppler anemometer in dilute sprays. 18th Annual Conf. on Liquid Atomization and Sprays Systems, Zaragoza, 2002
8. C. Fandrey, A. Naqwi, J. Shakal, H. Zhang, A Phase Doppler System for High Concentration Sprays. 10th International Symposium on Applications of Laser Techniques, Lisbon, 2000.

Nomenclature

N_D	particle number density (m^{-3})
D	particle diameter (m)
τ	optical length
x, y	Cartesian coordinates (m)
r	distance from the origin of the coordinates to the measuring point (m)